

Turning a Killing Mechanism into an Adhesion and Antifouling Advantage

Sarah Dedisch, Fabian Obstals, Andres de los Santos Pereira, Michael Bruns, Felix Jakob, Ulrich Schwaneberg,* and Cesar Rodriguez-Emmenegger*

Mild and universal methods to introduce functionality in polymeric surfaces remain a challenge. Herein, a bacterial killing mechanism based on amphiphilic antimicrobial peptides is turned into an adhesion advantage. Surface activity (surfactant) of the antimicrobial liquid chromatography peak I (LCI) peptide is exploited to achieve irreversible binding of a protein–polymer hybrid to surfaces via physical interactions. The protein–polymer hybrid consists of two blocks, a surface-affine block (LCI) and a functional block to prevent protein fouling on surfaces by grafting antifouling polymers via single electron transfer-living radical polymerization (SET-LRP). The mild conditions of SET-LRP of *N*-2-hydroxy propyl methacrylamide (HPMA) and carboxybetaine methacrylamide (CBMAA) preserve the secondary structure of the fusion protein. Adsorption kinetics and grafting densities are assessed using surface plasmon resonance and ellipsometry on model gold surfaces, while the functionalization of a range of artificial and natural surfaces, including teeth, is directly observed by confocal microscopy. Notably, the fusion protein modified with poly(HPMA) completely prevents the fouling from human blood plasma and thereby exhibits a resistance to protein fouling that is comparable to the best grafted-from polymer brushes. This, combined with their simple application on a large variety of materials, highlights the universal and scalable character of the antifouling concept.

implants, biosensors, medical devices,^[1] and a plethora of other applications.^[2] However, this proved challenging because of the need of specific functionalization to address the vastly different surface chemistry of different materials. In particular, those materials based on relatively inert polymers are difficult to modify and current strategies usually rely on harsh treatments such as oxidation with plasma or other oxidant reagents.^[3] Other chemical strategies include the use of comb polymers bearing antifouling poly(ethylene glycol) (PEG) or oxazolines and photo- or thermally addressable groups for C–C insertion reactions or functionalization of polydopamine (PDA) films with various polymers.^[4] More recently, polymer grafting on PDA coatings was achieved in a simplified approach where a ω -(dihydroxyphenyl ethylamino) poly(carboxybetaine) was mixed with dopamine prior dopamine polymerization.^[5] Their application in medical settings remains minor, presumably due to their complexity.^[6]

Functional materials play a key role in modern life due to their broad range of applications and versatile properties. Particularly, controlling interactions between artificial surfaces in contact with biological surroundings is key for the success of biomaterials,

implants, biosensors, medical devices,^[1] and a plethora of other applications.^[2] However, this proved challenging because of the need of specific functionalization to address the vastly different surface chemistry of different materials. In particular, those materials based on relatively inert polymers are difficult to modify and current strategies usually rely on harsh treatments such as oxidation with plasma or other oxidant reagents.^[3] Other chemical strategies include the use of comb polymers bearing antifouling poly(ethylene glycol) (PEG) or oxazolines and photo- or thermally addressable groups for C–C insertion reactions or functionalization of polydopamine (PDA) films with various polymers.^[4] More recently, polymer grafting on PDA coatings was achieved in a simplified approach where a ω -(dihydroxyphenyl ethylamino) poly(carboxybetaine) was mixed with dopamine prior dopamine polymerization.^[5] Their application in medical settings remains minor, presumably due to their complexity.^[6]

On the other hand, microorganisms have developed strategies to interact with interfaces to warrant their survival. For instance they produce antimicrobial amphiphilic peptides that can insert in the membranes of other microorganisms, destabilize them causing burst or lysis.^[7] The insertion is based on the amphiphilicity

S. Dedisch, F. Obstals, Dr. F. Jakob, Prof. U. Schwaneberg, Dr. C. Rodriguez-Emmenegger
 DWI-Leibniz Institute for Interactive Materials
 Forckenbeckstraße 50, D-52074 Aachen, Germany
 E-mail: schwaneberg@dwI.rwth-aachen.de;
 rodriguez@dwI.rwth-aachen.de

S. Dedisch, Dr. F. Jakob, Prof. U. Schwaneberg
 Lehrstuhl für Biotechnologie
 RWTH Aachen University
 Worringerweg 3, D-52074 Aachen, Germany

 The ORCID identification number(s) for the author(s) of this article can be found under <https://doi.org/10.1002/admi.201900847>.

© 2019 The Authors. Published by WILEY-VCH Verlag GmbH & Co. KGaA, Weinheim. This is an open access article under the terms of the Creative Commons Attribution License, which permits use, distribution and reproduction in any medium, provided the original work is properly cited.

Dr. A. de los Santos Pereira
 Department of Chemistry and Physics of Surfaces and Biointerfaces
 Institute of Macromolecular Chemistry
 Academy of Sciences of the Czech Republic
 Heyrovsky Square 2, 162 06 Prague, Czech Republic

Dr. M. Bruns
 Institute for Applied Materials (IAM)
 and Karlsruhe Nano Micro Facility (KNMF)
 Karlsruhe Institute of Technology (KIT)
 Hermann-von-Helmholtz Platz 1, D-76344
 Eggenstein-Leopoldshafen, Germany

Dr. C. Rodriguez-Emmenegger
 Institute of Technical and Macromolecular Chemistry
 RWTH Aachen University
 Forckenbeckstraße 50, D-52074 Aachen, Germany

DOI: 10.1002/admi.201900847

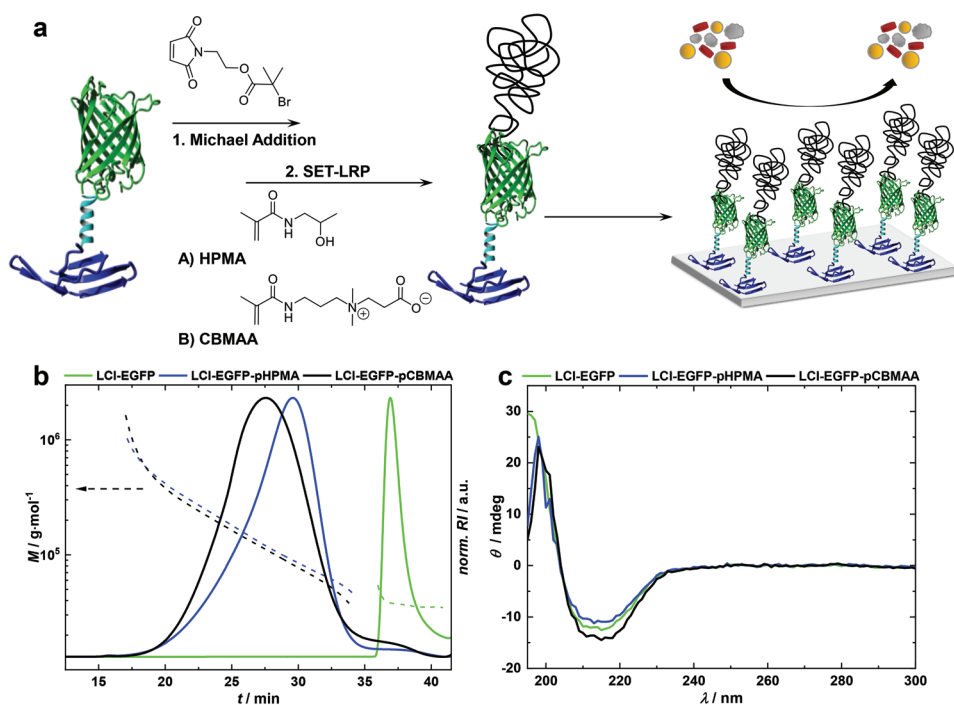


Figure 1. a) Schematic illustration of the functionalization route of LCI-EGFP grafted with poly(HPMA) and poly(CBMAA) and their resistance to blood plasma fouling. b) MALLS-SEC of the bare protein (green) and two protein–polymer hybrids: LCI-EGFP-pHPMA (blue) and LCI-EGFP-pCBMAA (black). The solid lines indicate the normalized refractive index change by time, while the dashed lines demonstrate the corresponding molecular weight. c) Circular dichroism spectra of LCI-EGFP (green) and both protein–polymer hybrids: LCI-EGFP-pHPMA (blue) and LCI-EGFP-pCBMAA (black).

of the peptide, which can adapt its conformation to expose those aminoacid residues that maximize the physical interactions with membrane components. The same principle can be utilized to functionalize virtually any interface.^[8] This mechanism is ubiquitous in the process of fouling.^[1b,9] Compared to other amphiphiles, antimicrobial peptides do not form higher order aggregates such as micelles, which would severely hamper the process of diffusion and adsorption towards surfaces. Although proteins such as albumin are commonly used for coating surfaces, such coatings may not be stable^[10] and their functionality may be ill-defined due the tendency of proteins to change conformation upon adsorption and over time.^[11]

Herein, we utilize the process of fouling to introduce a universal way to bring functionalities to surfaces. The concept introduced here, is to synthesize hybrid macromolecules which consist of two blocks, a surface-affine block binding to materials by physical interactions and a functional block (Figure 1a). The surface-affine block is an amphiphilic antimicrobial peptide called liquid chromatography peak I (LCI) consisting of 47 amino acids from the microorganism *Bacillus subtilis*. It comprises four antiparallel β -sheets resulting in a 3D structure with high thermal stability and it can exert hydrogen bonding (23 aminoacid residues, hydrophobic interactions, ionic interactions via positively charged C-terminus).^[12] The surface affine block LCI and enhanced green fluorescent protein (EGFP) were produced as a fusion protein in *Escherichia coli* BL21 Gold (DE3) cells and purified via chromatography (Supporting Information). The functional block consists of a green fluorescent protein (EGFP, genetically fused to LCI) from which (3-methacryloylamino-propyl)-(2-carboxy-ethyl)

dimethylammonium (carboxybetaine methacrylamide (CBMAA)) or *N*-(2-hydroxypropyl) methacrylamide (HPMA) chains are grafted. The EGFP is used as a fluorescent reporter to facilitate the proof that the hybrid macromolecule is attached to surfaces. Moreover, it offers two cysteine residues (position 69 and 91 of the EGFP) for the conjugation of a maleimide-functional initiator, 2-(2,5-dioxo-2,5-dihydro-1H-pyrrol-1-yl) ethyl 2-bromo-2-methylpropanoate, which was introduced by Michael addition. Therefrom, poly(HPMA) and poly(CBMAA) chains were grafted. These polymers were selected due to their unmatched resistance to protein fouling, lack of activation of coagulation and prevention of bacterial adhesion, three of the most sought properties in biomaterials.^[1b,13] Thus, the blocks of the hybrid molecules are antagonistic in nature but combined can bring unique synergistic functionalities to surfaces. HPMA and CBMAA were polymerized using single electron transfer-living radical polymerization (SET-LRP). SET-LRP is a relatively new type of polymerization which affords fast reaction rates and provides quantitative monomer conversion with high end-group fidelity due to nearly complete suppression of termination reactions.^[14] It was established as a robust and highly advantageous polymerization technique in aqueous systems,^[1a,15] but also decreasing the amount of copper catalyst compared to atom transfer radical polymerization (ATRP). SET-LRP is particularly advantageous for (meth)acrylamide monomers compared to ATRP. While the former led to conversions in excess of 90% in 15 h for *N*-2-hydroxypropyl methacrylamides,^[16] the latter only shows 19% in 23 h.^[17] Remarkably, it can be performed in rather facile conditions accessible to any chemical laboratory.^[18]

In this work, HPMA and CBMAA polymers were grafted from the LCI-EGFP at room temperature in phosphate buffered saline (PBS) utilizing a copper wire previously activated with hydrazine as catalyst. The conversions for the polymerization of poly(HPMA) and poly(CBMAA) were calculated to be between 80 and 97% by $^1\text{H-NMR}$ spectroscopy (Table S2, Supporting Information). Additionally, a substantial increase of the molecular weight was observed by multiangle laser-light scattering size exclusion chromatography (MALLS-SEC). The molecular weight of the protein increased from $37\,700\text{ g mol}^{-1}$ ($\text{PDI} = 1.004$) to the corresponding molecular weights of $126\,900$ and $129\,400\text{ g mol}^{-1}$ for the poly(HPMA) and poly(CBMAA) hybrids, respectively (Figure 1b). Remarkably, the polydispersity of the hybrid macromolecules only slightly increased ($\text{PDI} = 1.232$ for poly(HPMA) and $\text{PDI} = 1.229$ for poly(CBMAA)) even though the molecular weight quadruplicated. We wondered whether the polymers were grafted from both cysteine residues or from only one. Computational modeling suggested that the cysteine residue in position 91 is buried and not accessible for polymerization (Figure S1, Supporting Information). We confirmed this by performing the polymerization with a modified protein in which the cysteine at position 69 (accessible) is substituted for a serine. No polymer could be grafted from this protein proving that only the initiator attached to position 69 is available for polymerization.

It is noteworthy that grafting the polymers directly from the protein did not affect the secondary structure of the construct as evidenced by the maintenance of the fluorescence of EGFP and in the circular dichroism (CD) spectra (Figure 1c). The antimicrobial peptide LCI consists of four antiparallel β -sheets and the green fluorescent protein EGFP shows eleven β -sheets. Such β -sheets appear with negative bands at 218 nm and positive bands at 195 nm. Grafting of polymer did not affect the position nor the intensity of these bands.

The surface modification consisted of molecular adsorption of the protein-polymer hybrids (2.4 mg mL^{-1}) from a buffer solution. Coupons of poly(styrene) (PS), poly(4-methyl-1-pentene) (PMP), poly(dimethyl siloxane) (PDMS), and gold-coated substrates were incubated for 1 h without shaking to allow the protein-polymer hybrids to diffuse and bind onto the surface. These surfaces were selected due to their relevance in the biomedical field including membranes of oxygenators,^[19] contact lenses,^[20] microfluidics,^[21] and packaging material.^[22] The chemical composition of the coatings was assessed by X-ray photoelectron spectroscopy (XPS). Figure 2a,b depict the high-resolution C 1s (left) and N 1s (right) spectra of PMP before and after modification. XPS spectra of other surfaces can be found in Figures S3 and S4 of the Supporting Information. For the bare PMP substrate, the C 1s spectrum shows a single component at 285 eV arising from C-C, C-H, as expected from the chemical structure of the poly(4-methyl-1-pentene) membrane.^[23] Adsorption of LCI-EGFP (Figure 2a: B2) or the corresponding protein-polymer hybrids (Figure 2a: B3 and B4) leads to an increase in the signals of C-N, C-O, and N-C=O at 285.8, 286.6, and 288.2 eV not present in the spectrum of bare PMP (Figure 2a: B1).^[13c] The presence of these components is in good agreement with the protein and the polymer chemical structures. Importantly, a strong presence of amide in the spectra of the modified membranes has its origin in the

peptide bonds of the protein as well as in the polymer backbone of poly(HPMA) and poly(CBMAA). The strong contribution of C-C, C-H even in the surfaces after adsorption of the protein and protein-polymer hybrids arises partially from the underlying membrane substrate, indicating that the thickness of the surface modifications are lower than the analysis depth of XPS (up to 10 nm). Moreover, the amide binding is clearly evidenced in the N 1s region (Figure 2b), while a quaternary ammonium component also arises at 402.6 eV of LCI-EGFP-pCBMAA (Figure 2b: B4), confirming the chemical structure.^[9c] Thus, these results demonstrate that PMP was successfully modified with our protein-polymer hybrids.

The amount of protein adsorbed to the surface was quantified using surface plasmon resonance (SPR) spectroscopy. The adsorption kinetics were studied by flowing a protein solution of 2.4 mg mL^{-1} in PBS. Adsorption begins immediately upon contact with the surface reaching the saturation values at 75 min (Figure 2c). The bare protein adsorbed on gold is 395 ng cm^{-2} which is close to the values reported for the adsorption of a full monolayer of proteins.^[24] The binding of the protein-polymer hybrids resulted in similar adsorption curves. The adsorbed mass was calculated to be 209 and 325 ng cm^{-2} for the poly(HPMA) and poly(CBMAA) hybrids, respectively. It is remarkable that such high levels of functionalization could be readily achieved working with diluted water-borne solutions without any additional chemical reaction. The dry ellipsometric thicknesses were determined to be 2.53 nm for the bare protein and decreased to 2.04 and 1.74 nm, respectively, for the poly(HPMA) and poly(CBMAA) hybrids. The density of molecules at the surface can be assessed using the ellipsometric thickness (Equation (1)) or using the mass from SPR (Equation (2), summarized in Table 1). The former gives access to the dehydrated density, while the latter to the swollen state. The grafting density of bare protein is about 3–4 times larger than the protein-polymer hybrids. This might be caused by the larger excluded volume effects (larger cross-section of the protein-polymer hybrids with larger R_H) and by the competition between the free energy of binding (driving force for adsorption) and the osmotic pressure increase (entropic repulsion).^[25] Interestingly, the grafting density for LCI-EGFP-pCBMAA was higher than LCI-EGFP-pHPMA in swollen state while in dry state the opposite was observed. Such seemingly confronting results are caused by the much larger swelling of poly(CBMAA) compared to poly(HPMA).

Shear stress can pose challenges to coatings by causing its erosion.^[26] To assess the potential effect of shear on the stability of the brushes, the changes of mass of adsorbed protein-polymer hybrids were monitored via SPR as a function of the flow rate in the range of $6\text{--}500\text{ }\mu\text{L min}^{-1}$ in PBS at $25\text{ }^\circ\text{C}$. The Reynolds numbers for all the flow conditions were below 0.7, which indicates that the flow was in the laminar regime ($\text{Re} < 1900$). The shear stress at the wall was estimated to be in a range from 4.5 to 380 mPa (Figure 2d; Figure S1, Supporting Information). The low range of shear stress can be found in urinary catheters, contact lenses as well as peroneal veins, while the higher shears stresses are typically observed in kidney ducts and heart valves.^[27] No detachment of the protein-polymer hybrids was observed in spite of the 85-fold increase in shear stress, indicating the high stability of the coating.

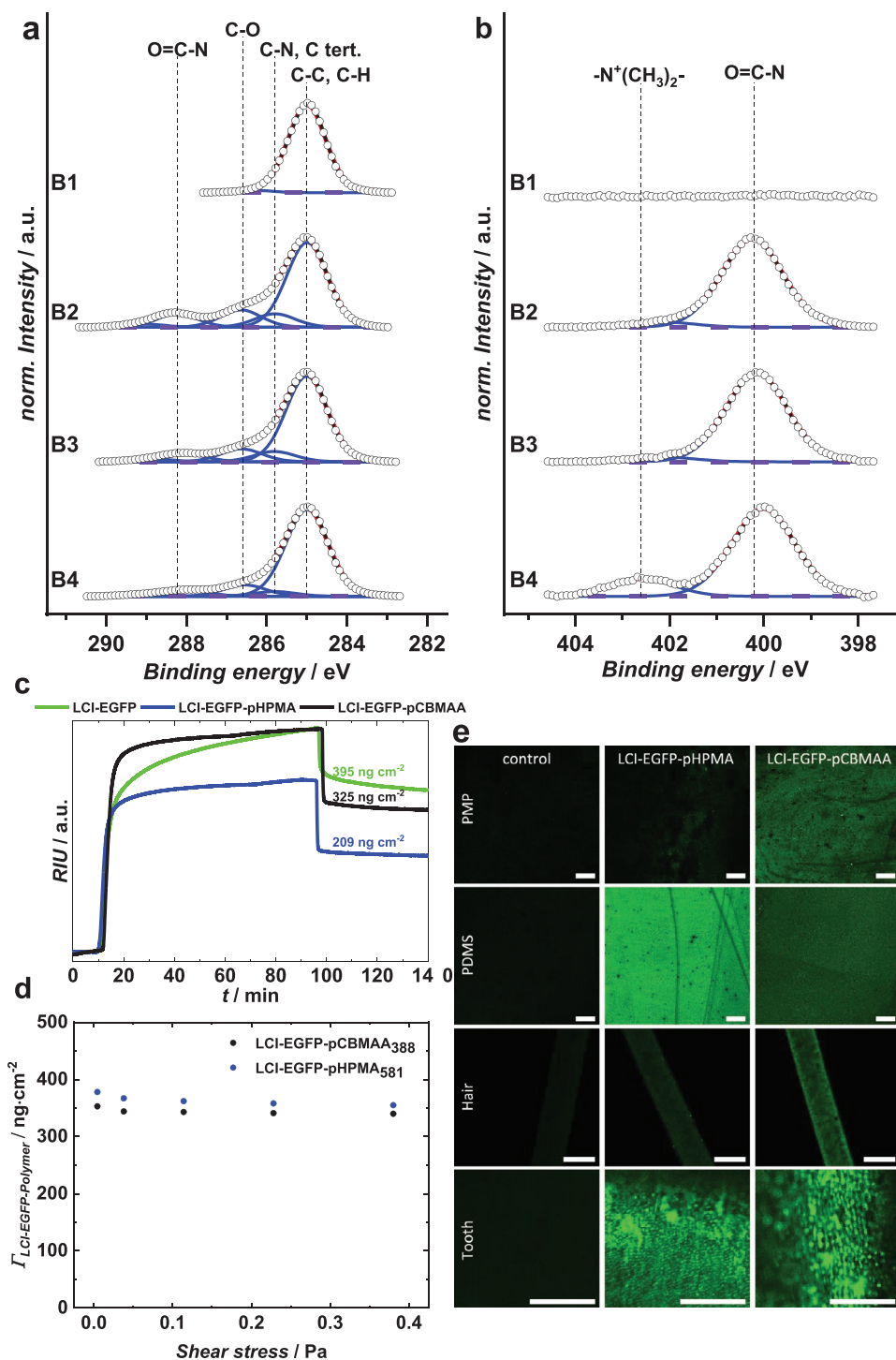


Figure 2. High-resolution a) C 1s and b) N 1s XPS spectra of the surface modifications on PMP. The different modifications are numbered and correspond to: (1) bare PMP, (2) LCI-EGFP, (3) LCI-EGFP-pHPMA, and (4) LCI-EGFP-pCBMAA. For a better visualization all spectra were normalized to maximum intensity. c) SPR sensograms of the adsorption of LCI-EGFP (green) and both protein–polymer hybrids: LCI-EGFP-pHPMA (blue) and LCI-EGFP-pCBMAA (black). d) Density of adsorbed protein–polymer hybrids at different shear stresses monitored by SPR. The experiment was performed by flowing PBS in the range of 6–500 $\mu\text{L min}^{-1}$ at 25 °C. e) Confocal images of surface modifications of LCI-EGFP-pHPMA, LCI-EGFP-pCBMAA, and EGFP as control, on PMP, PDMS, hair, and tooth. The scale bars represent 100 μm .

Moreover, we explored the binding of the protein–polymer hybrids to other surfaces using confocal microscopy (Figure 2e; Figure S2, Supporting Information). The green fluorescence of EGFP was used as fluorescent reporter to qualitatively assess the

binding of the protein–polymer hybrids to PMP, PDMS, hair, and teeth (Figure 2e). LCI-EGFP-pHPMA and LCI-EGFP-pCBMAA (both) attached to all tested surfaces (Figure S2, Supporting Information). Conversely, negligible fluorescence was observed on the

Table 1. Ellipsometric thickness and grafting densities calculated for the bare protein and the protein–polymer hybrid samples.

Sample	Thickness [nm]	$\sigma_{\text{ellips.}}^{\text{a)}} [\text{nm}^{-2}]$	$\sigma_{\text{SPR}}^{\text{b)}} [\text{nm}^{-2}]$
LCI-EGFP	2.53	0.0405	0.0632
LCI-EGFP-pHPMA	2.04	0.0119	0.0122
LCI-EGFP-pCBMAA	1.72	0.00981	0.0186

The grafting density was calculated in two ways: $\sigma_{\text{ellips.}}^{\text{a)}} = \frac{h_{\text{ellips.}} \cdot \rho \cdot N_{\text{A}}}{M_{\text{n}}}$ (1) where $h_{\text{ellips.}}$ is dry ellipsometric thickness, ρ is bulk density, N_{A} is Avogadro constant, and M_{n} is number average molecular weight; $\sigma_{\text{SPR}}^{\text{b)}} = \frac{\Delta m_{\text{SPR}} \cdot N_{\text{A}}}{M_{\text{n}}}$ (2) where Δm_{SPR} is mass adsorbed per unit area obtained from SPR.

negative control after contact with bare EGFP. Moreover, the protein–polymer hybrids bound to highly complex natural materials such as hair (a protein filament consisting of α -keratin), and teeth, a hard calcified structure (Figure 2e). The ease of modification of such diverse and challenging surfaces, including surfaces of teeth and hair, highlight the potential of this coating strategy to design and introduce chemical and biochemical functionalities which could even be performed directly in the human body. A quantitative comparison in the binding efficiency between LCI-EGFP-pHPMA and LCI-EGFP-pCBMAA on such complex samples cannot be accurately done due to the difficulties in maintaining equivalent optical conditions between samples with different roughness and thickness such as tooth cuts.

As an example of an application we studied the fouling from human blood plasma (BP, 10% in PBS) and its main protein human serum albumin (HSA, 5 mg mL⁻¹) on the coatings deposited on model gold surfaces using SPR. Protein adsorption from blood plasma is a ubiquitous process occurring on all surfaces different from healthy endothelium.^[28] The protein–polymer hybrid coatings prevented the fouling from HSA compared to gold (fouling 92 ng cm⁻², Figure 3a). However, a reduction or even prevention of the adsorption of HSA does not render the surface resistant to BP.^[1b] BP is responsible for a much larger fouling on bare gold accounting for approximately 300 ng cm⁻². The adsorption of the LCI-EGFP reduced the fouling from BP in a similar way other proteins are used to passivate surfaces. However, this is not enough for real applications such as biomaterials and medical devices, where the remaining amount of fouling could still lead to complications such as poor biocompatibility. Remarkably, LCI-EGFP-pCBMAA and LCI-EGFP-pHPMA coatings with a degree of polymerization (DP) of 388 and 376 reduced the fouling by 86% and 82%, respectively. Increasing the DP to 640 and 776 for HPMA and CBMAA further decreased the fouling by more than 95% and 88%, respectively (Figure 3a). Such impressive reduction of fouling is well in line with our previous results of polymer brushes of the same monomers grafted directly from the substrate.^[1b,13d] Compared to the grafting-from of brushes, the approach introduced in this work can be readily applicable to obtain antifouling coatings by personnel without intensive training in chemistry and we foresee its application in medical fields.

In summary, we turned an a priori negative process—the adsorption of an antimicrobial peptide—into a universal tool to introduce functionality to the surface of natural and synthetic materials. The approach relies on the physisorption of the surface affine block which carries antifouling polymers. In contrast

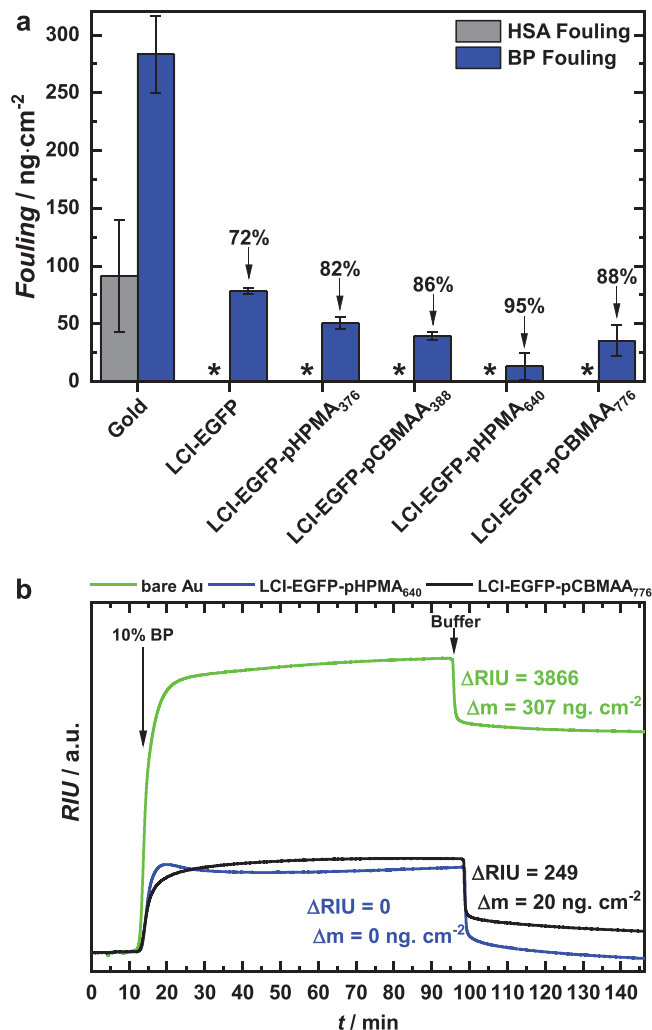


Figure 3. a) HSA and BP fouling, measured via SPR spectroscopy, on different surface modifications on a gold chip and b) SPR sensograms of the resistance to blood plasma fouling of an uncoated gold chip (green), a gold chip coated with LCI-EGFP-pHPMA₆₄₀ (blue), and a gold chip coated with LCI-EGFP-pCBMAA₇₇₆ (black). The fouling was measured by flowing blood plasma at 6 $\mu\text{L min}^{-1}$ and shear stress of 4.5 mPa. All samples were measured in triplicate.

to most of the well-known PDA coatings, which only introduce functional groups for further postmodification, our approach based on a hybrid macromolecule with a surface-affine and a functional domain introduced functionality in a single adsorption step of a single component. The coatings prepared reduced the fouling from blood plasma (10%) to same levels as polymer brushes, the gold-standard for antifouling surfaces. We envision that the excellent resistance to protein fouling and ease of application of the introduced coatings will pave their way to medical devices, where a tight control of the properties combined with a facile application results in a unique advantage.

Supporting Information

Supporting Information is available from the Wiley Online Library or from the author.

Acknowledgements

S.D. and F.O. contributed equally to this work. The authors acknowledge the financial support by the Deutsche Forschungsgemeinschaft (DFG, German Research Foundation) via Schwerpunktprogramm "Towards an Implantable Lung," Project Nos. 346972946 and 347367912 and the Federal Ministry of Education and Research of Germany (FKZ: 031B0104B). C.R.-E. acknowledges the Karlsruhe Nano Micro Facility for support in XPS characterization. The K-Alpha+ instrument was financially supported by the Federal Ministry of Economics and Technology on the basis of a decision by the German Bundestag. Moreover, Dr. Daniel Sauer is acknowledged for support in CD analytic. The authors acknowledge support of the Center for Chemical Polymer Technology (CPT) under the support of the EU and the federal state of North Rhine-Westphalia (Grant No. EFRE 30 00 883 02).

Conflict of Interest

The authors declare no conflict of interest.

Keywords

adhesion peptides, anchor peptides, antifouling, biomimetic coatings, SET-LRP

Received: May 13, 2019

Revised: June 21, 2019

Published online:

- [1] a) M. Vorobii, A. de los Santos Pereira, O. Pop-Georgievski, N. Y. Kostina, C. Rodriguez-Emmenegger, V. Percec, *Polym. Chem.* **2015**, *6*, 4210; b) C. Rodriguez-Emmenegger, E. Brynda, T. Riedel, M. Houska, V. Šubr, A. Bologna Alles, E. Hasan, J. E. Gautrot, W. T. S. Huck, *Macromol. Rapid Commun.* **2011**, *32*, 952.
- [2] B. D. Ratner, A. S. Hoffman, F. J. Schoen, J. E. Lemons, Academic Press, San Diego, CA **2004**.
- [3] M. Ozdemir, C. U. Yurteri, H. Sadikoglu, *Crit. Rev. Food Sci. Nutr.* **1999**, *39*, 457.
- [4] a) R. Konradi, C. Acikgoz, M. Textor, *Macromol. Rapid Commun.* **2012**, *33*, 1663; b) S. A. Al-Bataineh, R. Luginbuehl, M. Textor, M. Yan, *Langmuir* **2009**, *25*, 7432; c) O. Pop-Georgievski, C. Rodriguez-Emmenegger, A. de los Santos Pereira, V. Proks, E. Brynda, F. Rypacek, *J. Mater. Chem. B* **2013**, *1*, 2859.
- [5] H. S. Sundaram, X. Han, A. K. Nowinski, N. D. Brault, Y. Li, J.-R. Ella-Menye, K. A. Amoaka, K. E. Cook, P. Marek, K. Senecal, S. Jiang, *Adv. Mater. Interfaces* **2014**, *1*, 1400071.
- [6] A. Mysiak, M. Kobusiak-Prokopowicz, T. Kucharski, R. Kleczyk, *Pol. Merku. Lekarski* **2010**, *29*, 149.
- [7] a) K. A. Brogden, *Nat. Rev. Microbiol.* **2005**, *3*, 238; b) L. T. Nguyen, E. F. Haney, H. J. Vogel, *Trends Biotechnol.* **2011**, *29*, 464.
- [8] a) M. Noor, T. Dworeck, A. Schenk, P. Shinde, M. Fioroni, U. Schwaneberg, *J. Biotechnol.* **2012**, *157*, 31; b) K. Rübsam, B. Stomps, A. Böker, F. Jakob, U. Schwaneberg, *Polymer* **2017**, *116*, 124; c) K. Rübsam, L. Weber, F. Jakob, U. Schwaneberg, *Biotechnol. Bioeng.* **2018**, *115*, 321; d) K. Rübsam, M. Davari, F. Jakob, U. Schwaneberg, *Polymers* **2018**, *10*, 423; e) M. Meißler, A. Taden, H. G. Börner, *ACS Macro Lett.* **2016**, *5*, 583; f) G. P. Sakala, M. Reches, *Adv. Mater. Interfaces* **2018**, *5*, 1800073.
- [9] a) C. Rodriguez-Emmenegger, E. Brynda, T. Riedel, Z. Sedlakova, M. Houska, A. B. Alles, *Langmuir* **2009**, *25*, 6328; b) T. Riedel, Z. Riedelová-Reichelová, P. Májek, C. Rodriguez-Emmenegger, M. Houska, J. E. Dyr, E. Brynda, *Langmuir* **2013**, *29*, 3388; c) F. Surman, T. Riedel, M. Bruns, N. Y. Kostina, Z. Sedláková, C. Rodriguez-Emmenegger, *Macromol. Biosci.* **2015**, *15*, 636.
- [10] C. M. Nelson, S. Raghavan, J. L. Tan, C. S. Chen, *Langmuir* **2003**, *19*, 1493.
- [11] a) B. Sivaraman, R. A. Latour, *Langmuir* **2012**, *28*, 2745; b) L. Vroman, A. L. Adams, *J. Colloid Interface Sci.* **1986**, *111*, 391; c) L. Vroman, *Colloids Surf., B* **2008**, *62*, 1.
- [12] W. Gong, J. Wang, Z. Chen, B. Xia, G. Lu, *Biochemistry* **2011**, *50*, 3621.
- [13] a) Z. Zhang, T. Chao, S. Chen, S. Jiang, *Langmuir* **2006**, *22*, 10072; b) Z. Wu, H. Chen, X. Liu, Y. Zhang, D. Li, H. Huang, *Langmuir* **2009**, *25*, 2900; c) G. Cheng, G. Li, H. Xue, S. Chen, J. D. Bryers, S. Jiang, *Biomaterials* **2009**, *30*, 5234; d) A. de los Santos Pereira, S. Sheikh, C. Blaszykowski, O. Pop-Georgievski, K. Fedorov, M. Thompson, C. Rodriguez-Emmenegger, *Biomacromolecules* **2016**, *17*, 1179; e) C. Rodriguez-Emmenegger, S. Janel, A. de los Santos Pereira, M. Bruns, F. Lafont, *Polym. Chem.* **2015**, *6*, 5740.
- [14] a) X. Jiang, B. M. Rosen, V. Percec, *J. Polym. Sci., Part A: Polym. Chem.* **2010**, *48*, 2716; b) N. H. Nguyen, M. E. Levere, J. Kulis, M. J. Monteiro, V. Percec, *Macromolecules* **2012**, *45*, 4606; c) N. H. Nguyen, M. E. Levere, V. Percec, *J. Polym. Sci., Part A: Polym. Chem.* **2012**, *50*, 860; d) A. H. Soeriyadi, C. Boyer, F. Nyström, P. B. Zetterlund, M. R. Whittaker, *J. Am. Chem. Soc.* **2011**, *133*, 11128.
- [15] a) G. Lligadas, S. Grama, V. Percec, *Biomacromolecules* **2017**, *18*, 2981; b) M. Vorobii, O. Pop-Georgievski, A. de los Santos Pereira, N. Y. Kostina, R. Jezorek, Z. Sedláková, V. Percec, C. Rodriguez-Emmenegger, *Polym. Chem.* **2016**, *7*, 6934.
- [16] N. H. Nguyen, C. Rodriguez-Emmenegger, E. Brynda, Z. Sedlakova, V. Percec, *Polym. Chem.* **2013**, *4*, 2424.
- [17] M. Teodorescu, K. Matyjaszewski, *Macromol. Rapid Commun.* **2000**, *21*, 190.
- [18] a) E. Liarou, A. Anastasaki, R. Whitfield, C. E. Iacono, G. Patias, N. G. Engelis, A. Marathianos, G. R. Jones, D. M. Haddleton, *Polym. Chem.* **2019**, *10*, 963; b) G. Lligadas, S. Grama, V. Percec, *Biomacromolecules* **2017**, *18*, 1039.
- [19] D. N. Gray, *Polymeric Materials and Artificial Organs*, Vol. 256, American Chemical Society, Washington, DC **1984**, pp. 151–162.
- [20] P. C. Nicolson, J. Vogt, *Biomaterials* **2001**, *22*, 3273.
- [21] a) J. M. Goddard, J. H. Hotchkiss, *Prog. Polym. Sci.* **2007**, *32*, 698; b) D. F. Stamatialis, B. J. Papenburg, M. Gironés, S. Saiful, S. N. M. Bettahalli, S. Schmitmeier, M. Wessling, *J. Membr. Sci.* **2008**, *308*, 1.
- [22] J. Miltz, V. Rosen-Doody, *J. Food Process. Preserv.* **1985**, *8*, 151.
- [23] F. Obstals, M. Vorobii, T. Riedel, A. de los Santos Pereira, M. Bruns, S. Singh, C. Rodriguez-Emmenegger, *Macromol. Biosci.* **2018**, *18*, 1700359.
- [24] C. Rodriguez-Emmenegger, O. Kylián, M. Houska, E. Brynda, A. Artemenko, J. Kousal, A. B. Alles, H. Biederman, *Biomacromolecules* **2011**, *12*, 1058.
- [25] M. Rubinstein, R. H. Colby, *Polymer Physics*, Oxford University Press, Oxford **2003**.
- [26] A. Belanger, A. Decarmine, S. Jiang, K. Cook, K. A. Amoako, *Langmuir* **2019**, *35*, 1984.
- [27] B. Lopez-Mila, P. Alves, T. Riedel, B. Dittrich, F. Mergulhão, C. Rodriguez-Emmenegger, *Bioinspiration Biomimetics* **2018**, *13*, 065001.
- [28] M. Thompson, C. Blaszykowski, S. Sheikh, C. Rodriguez-Emmenegger, A. de los Santos Pereira, *Biological Fluid-Surface Interactions in Detection and Medical Devices*, Royal Society of Chemistry, London **2017**.